

## Article

# Gas-Graft Coverage After DMEK: A Clinically Validated Numeric Study

Jan O. Pralits<sup>1,\*</sup>, Mark Alberti<sup>2,\*</sup>, and Javier Cabreizo<sup>2,3</sup>

<sup>1</sup> Department of Civil, Chemical and Environmental Engineering, University of Genoa, Italy

<sup>2</sup> Department of Ophthalmology, Rigshospitalet, Glostrup, Denmark

<sup>3</sup> Copenhagen Eye Foundation, Copenhagen, Denmark

**Correspondence:** Mark Alberti, Department of Ophthalmology, Rigshospitalet – Glostrup, Valdemar Hansen Vej 13, 2600 Glostrup, Denmark. e-mail: markalberti@gmail.com

**Received:** 22 April 2019

**Accepted:** 1 September 2019

**Published:** 12 November 2019

**Keywords:** endothelial keratoplasty; intraocular gas; patient positioning; numeric model; DMEK

**Citation:** Pralits JO, Alberti M, Cabreizo J. Gas-graft coverage after DMEK: a clinically validated numeric study. *Trans Vis Sci Tech.* 2019;8(6):9. <https://doi.org/10.1167/tvst.8.6.9> Copyright 2019 The Authors

**Purpose:** We investigate the influence of positioning, gas fill, and anterior chamber size on bubble configuration and graft coverage after Descemet's membrane endothelial keratoplasty (DMEK).

**Methods:** We use a mathematical model to study the bubble shape and graft coverage in eyes of varying anterior chamber depths (ACD). The governing equations are solved numerically using the open source software OpenFOAM. Numeric results are validated clinically so that clinical gas fill measures can be correlated with numeric results providing gas-graft coverage information otherwise clinically inaccessible.

**Results:** In a phakic eye (ACD = 2.65 mm) with a gas fill of 35%, graft contact ranged from 35% to 38% depending on positioning and increased to 85% to 92% with a 70% fill. In contrast, positioning of a pseudophakic eye (ACD = 4.35) with a gas fill of 35% results in graft contact ranging from 8% to 52%, increasing to 63% to 94% with a 70% fill. The mathematical model demonstrates negligible differences between air and SF6 results and interestingly, a very thin central patch of aqueous humor within the gas bubble is found in some cases.

**Conclusions:** Graft coverage in phakic eyes (ACD ≤ 3 mm) is dominated by the gas fill and less sensitive to patient positioning. In pseudophakic eyes with larger values of ACD, the graft coverage depends on gas fill and patient positioning with positioning even more important as ACD increases.

**Translational Relevance:** Anterior chamber depth markedly influences the role of patient positioning in gas-filled eyes after DMEK due to the interplay between anterior chamber anatomy and gas bubble morphology.

## Introduction

Descemet's membrane endothelial keratoplasty (DMEK) is increasingly becoming the treatment of choice for corneal endothelial dysfunction. As with other endothelial keratoplasty procedures, the use of air or gas in the anterior chamber (AC) is fundamental to sutureless adherence of the donor graft to the host cornea. Studies suggest that a larger bubble helps prevent graft detachment and rebubbling procedures<sup>1,2</sup> whereas gas overfill leads to complications, such as pupillary block<sup>3</sup> and raises concern of possible endothelial toxicity.<sup>4,5</sup> The ideal gas fill after DMEK to date is unknown and a lack of knowledge of air and gas behavior in the AC hinders optimal surgical

results. Therefore, a better understanding of how positioning and AC shape influence bubble configuration, and graft coverage, in the AC is needed. Furthermore, this understanding will allow us to examine relationships between one-dimensional bubble height, two-dimensional gas-graft contact, and three-dimensional gas volume. To this end, we have performed a numeric study of gas fill in model- and patient-specific ACs, including the DMEK graft. The shape of the gas bubble is computed for phakic and pseudophakic ACs, accounting for the properties of air, SF6 and aqueous humor (AH). For each geometry the gas coverage on the graft is computed for different values of the gas fill and patient positioning.

**Table 1.** Parameter Values for Two Phakic and Two Pseudophakic AC Geometries

Parameter	Abbreviation	Value
Geometrical characteristics of the phakic ACs		
Volume of the AC	$V_{AC}$	0.162/0.194 mL
Diameter of the AC	$D_{AC}$	12.5/12.5 mm
AC depth <sup>8</sup>	ACD	2.65/3.00 mm
Posterior cornea minimum radius of curvature <sup>9</sup>	$R_C$	6.8/6.8 mm
Radius of curvature of the natural lens	$R_L$	10.0/10.00 mm
Height of the iris–lens channel		0.1/0.1 mm
Angle between cornea and iris		30°/35°
Geometrical characteristics of the pseudophakic ACs		
Volume of the AC	$V_{AC}$	0.245/0.287 mL
Diameter of the AC	$D_{AC}$	12.7/12.7 mm
AC depth <sup>8</sup>	ACD	4.00/4.35 mm
Posterior cornea minimum radius of curvature <sup>9</sup>	$R_C$	6.8/6.8 mm
Radius of curvature of the natural lens	$R_L$	$\infty/\infty$
Height of the iris–lens channel		0.24/0.24 mm
Angle between cornea and iris		43°/53°

The results are presented graphically and show how to obtain gas-graft coverage and gas volume from clinical measures. Our objective is to map gas coverage of grafts for different gas fills and varying patient orientations and, thus, improve our understanding of gas use in the AC.

## Material and Methods

### Geometries of the AC

Idealized geometries of the AC have been used to model a phakic as well as a pseudophakic eye. The

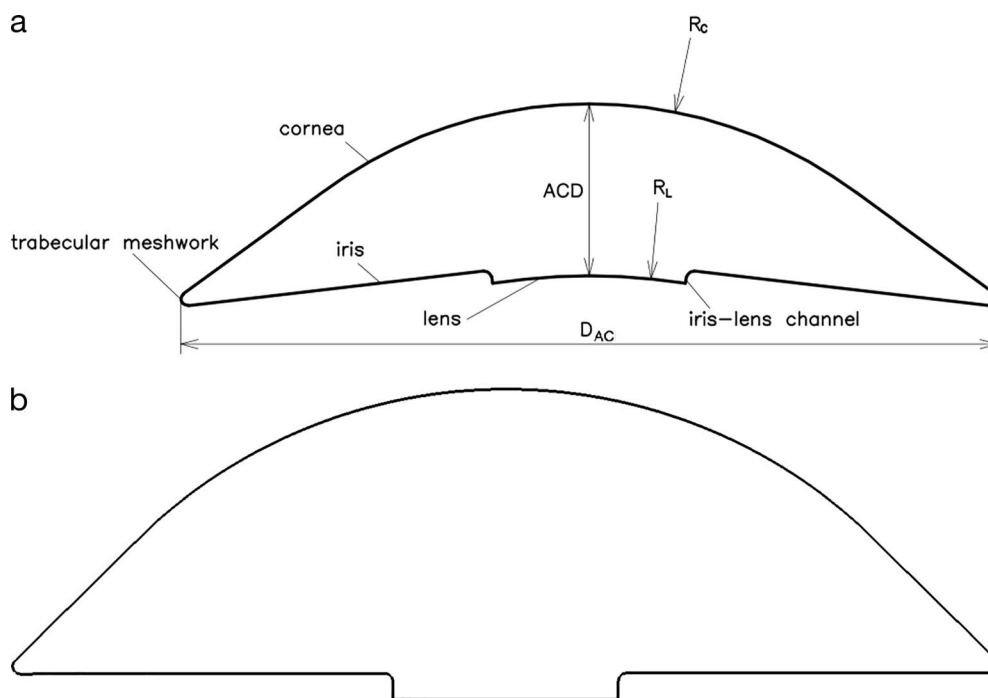


**Figure 1.** Symmetry plane of the AC geometries; (a) phakic eye including definition of dimensions, (b) pseudophakic eye. See Table 1 for abbreviations and parameter values.

**Table 2.** Parameter Values Used for Air, SF6, and Aqueous Humor in the Simulations

Parameter	Abbreviation	Value
Aqueous humor properties		
Density <sup>14</sup>	$\rho$	1000 kg/m <sup>3</sup>
Kinematic viscosity <sup>15</sup>	$\nu$	$7.5 \cdot 10^{-7}$ m <sup>2</sup> /s
Air properties		
Density <sup>14</sup>	$\rho$	1.225 kg/m <sup>3</sup>
Kinematic viscosity <sup>14</sup>	$\nu$	$1.5 \cdot 10^{-5}$ m <sup>2</sup> /s
Surface tension with aqueous <sup>14</sup>	$\sigma_{\text{air}}$	0.07 N/m
Iris contact angle	$\alpha_{\text{iris}}$	24°
Lens contact angle (phakic) <sup>16</sup>	$\alpha_{\text{lens}}$	24°
Lens contact angle (pseudo) <sup>17</sup>	$\alpha_{\text{lens}}$	45.9°
Cornea contact angle <sup>8</sup>	$\alpha_{\text{lens}}$	16.59° ± 3.20°
SF6 properties		
Density <sup>18</sup>	$\rho$	6.17 kg/m <sup>3</sup>
Kinematic viscosity <sup>19</sup>	$\nu$	$1.5 \cdot 10^{-5}$ m <sup>2</sup> /s
Surface tension with aqueous <sup>18</sup>	$\sigma_{\text{air}}$	0.07 N/m
Iris contact angle	$\alpha_{\text{iris}}$	24°
Lens contact angle (phakic) <sup>16</sup>	$\alpha_{\text{lens}}$	24°
Lens contact angle (pseudo) <sup>17</sup>	$\alpha_{\text{lens}}$	45.9°
Cornea contact angle <sup>8</sup>	$\alpha_{\text{lens}}$	16.81° ± 3.11°

model representing a phakic eye is based on the geometry used by Repetto et al.<sup>6</sup> (Fig. 1a). The geometry of the pseudophakic eye (Fig. 1b) has been taken from the investigation by Kapnisis et al.<sup>7</sup> The AC depth (ACD) values for the phakic and pseudophakic model were set to 2.65 and 4.35 mm, representing average ACD dimensions in the Fuch's endothelial dystrophy patient population eligible for endothelial keratoplasty procedures involving air/gas in the AC (see ClinicalTrials.gov identifier: NCT03407755).<sup>8</sup> Moreover, for comparison the

investigation also was conducted for a phakic AC with ACD = 3.00 mm and a pseudophakic AC with ACD = 4.00 mm. The geometric characteristics of the phakic and pseudophakic ACs are shown in Table 1 and Figure 1.

The patient-specific phakic AC model was constructed from dense anterior segment OCT (128 radial slices; CASIA2, Tomey Corp., Nagoya, Japan) from a patient scheduled for endothelial keratoplasty. Images were exported and points representing corneal endothelium, iris and lens were manually mapped using Fiji (based on ImageJ version 1.51s). Mapped points were imported into MATLAB (version R2016b; Mathworks Inc., Natick, MA) so a stereolithography (STL) file could be constructed, which describes the surface geometry of the three-dimensional AC. The AC STL-file could then be used in our numeric model for gas fill evaluations.

Clinical aspects of this study involving patients adheres in accordance with the tenets of the Declaration of Helsinki.

### Description of the model

The gas fill in the AC, and the corresponding gas coverage on the graft were computed numerically by solving the governing equations for mass conservation and momentum balance for two immiscible fluids

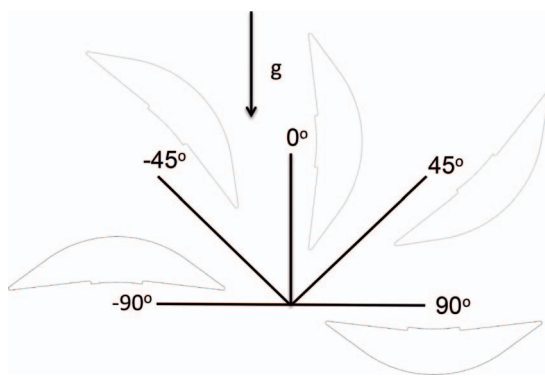


**Figure 2.** Definition of the positioning angle  $\psi$  of the patients with respect to the gravitational acceleration  $g$ . Thus,  $-90^\circ$  represents the face-up position and  $90^\circ$  represents the face-down position.

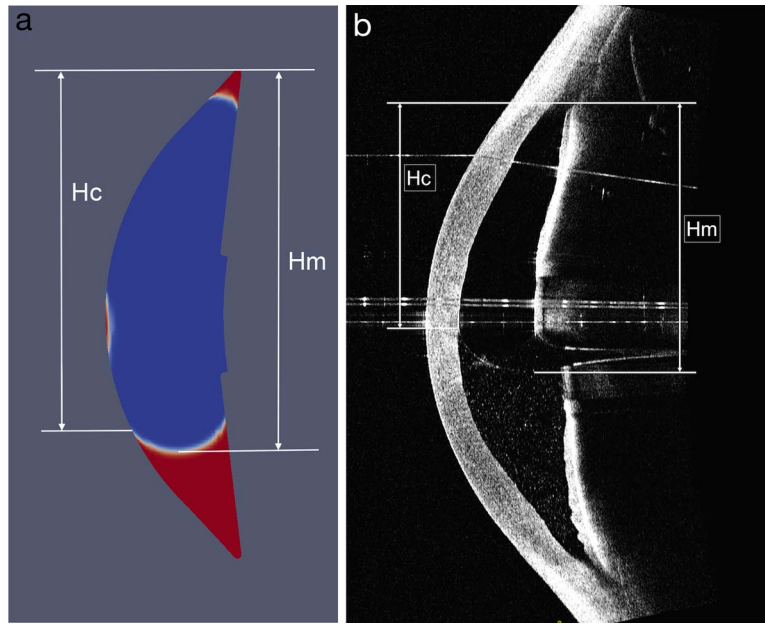


**Figure 3.** Definition of vertical height  $H_c$  from inferior gas-cornea contact to superior chamber angle and vertical height  $H_m$  from inferior bubble to superior chamber angle. Gravity is acting in the vertical direction, from top to bottom. (a) numeric model, (b) OCT image. Horizontal reflection lines are seen on the OCT image; however, these are artefacts due to the gas bubble in the eye.

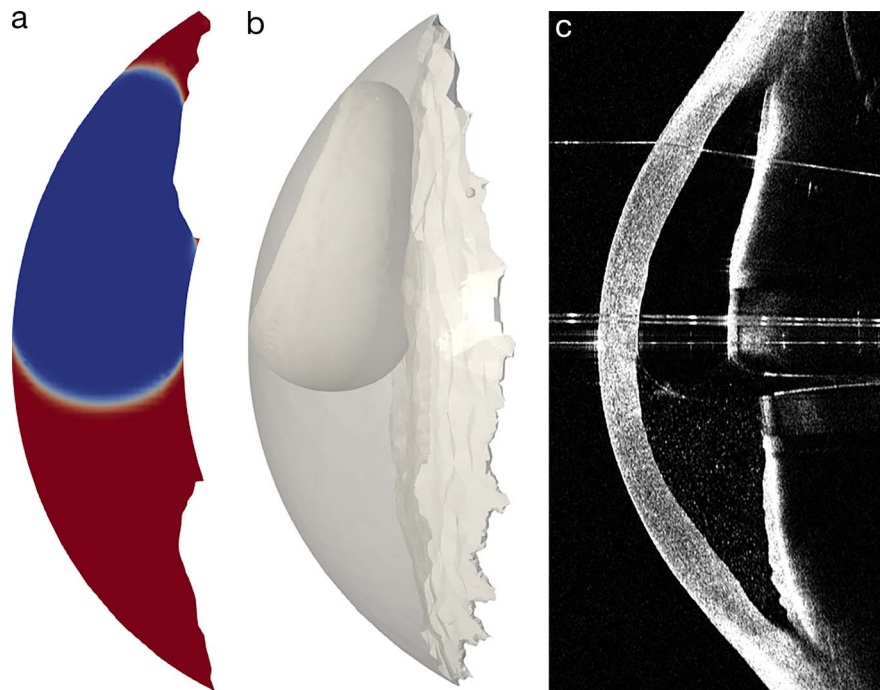


**Figure 4.** Patient specific phakic AC in side view; (a) numeric solution with aqueous humor in red, interface in white and air in blue for  $V_{air}/V_{AC} = 39.5\%$ ,  $H_c/D_{AC} = 49.4\%$  and  $H_m/D_{AC} = 58.4\%$  (ACD = 2.75 mm). (b) Three-dimensional reconstruction of the numeric solution; (c) OCT of a patient with gas in the AC;  $H_c/D_{AC} = 49.4\%$  and  $H_m/D_{AC} = 58.4\%$  (ACD = 2.75 mm). The interface is seen as a thin white contour. For all figures gravity acts downwards in the vertical direction.

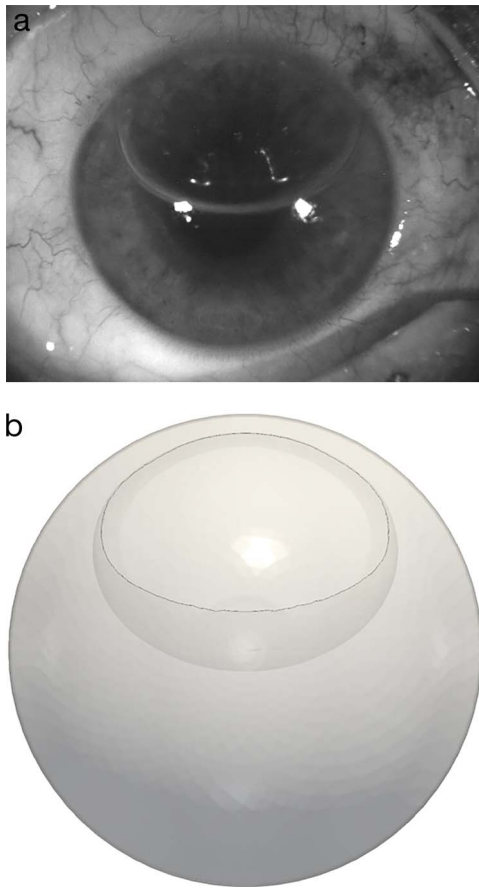


**Figure 5.** (a) Near-infrared image of patient with air in the AC (ACD = 2.75 mm). (b) Three-dimensional reconstruction of the numeric solution presented in Figures 4a and 4b.

throughout the domain, and the interface was tracked using the Volume of Fluid (VOF) method. The governing equations are given as:

$$\nabla \cdot U = 0, \quad (1)$$

$$\rho \frac{\partial U}{\partial t} + \rho U \cdot \nabla U - \mu \nabla^2 U = -\nabla p_d - \rho g \cdot x + \sigma \kappa \nabla \gamma, \quad (2)$$

where  $U$  is the fluid velocity,  $\rho$  density,  $\mu$  dynamic viscosity,  $p_d$  pressure,  $g$  gravitational acceleration,  $\sigma$  surface tension,  $\kappa$  interface curvature, and  $\gamma$  an indicator function representing the volume fraction of one fluid phase. The two immiscible fluids are considered as one effective fluid throughout the domain. Their physical properties are calculated as weighted averages based on the distribution of the liquid volume fraction, thus being equal to the properties of each fluid ( $U, \rho, \mu$ ) in their corresponding occupied regions and varying only across the

interface;  $X = X_l \gamma + X_g(1 - \gamma)$ , where  $X$  is a generic property and subscripts  $l$  and  $g$  represent the liquid and gas phase, respectively.

The volume fraction of each fluid phase was solved using the VOF method,<sup>10,11</sup> which relies on the solution of a transport equation for  $\gamma$ , which can be written

$$\frac{\partial \gamma}{\partial t} + \nabla \cdot (U\gamma) + \nabla \cdot (U_r(1 - \gamma)) = 0 \quad (3)$$

The phase fraction  $\gamma$  can take values within the range  $0 \leq \gamma \leq 1$ , with the values of zero and one corresponding to regions accommodating only one phase; for example,  $\gamma = 0$  for the gas and  $\gamma = 1$  for the liquid. The term proportional to the relative velocity  $U_r = U_l - U_g$  is active only in the interface region and increases the interface resolution; thus, avoiding special numeric treatment. Numeric simulations are performed using the free software OpenFOAM (OpenCFD Ltd, available in the public domain at <http://openfoam.com>). The snappyHexMesh tool by OpenFOAM is used to make the meshes, which produces unstructured meshes consisting of tetragonal and hexahedral volumes. We used on average 1.2 million volumes to perform three-dimensional (3D) simulations and run the code in parallel on a 36-processor computer at the high-performance computing center CINECA (Bologna, Italy). Before the simulations, careful mesh-independence tests have been made. The numeric simulations are run by fixing the volume ratio (ratio of the gas volume to the total volume of the domain) and setting an initially flat and horizontal shape of the interface. Advancing in time, the interface evolves towards its equilibrium shape; when a steady solution is obtained, the simulation ends. The viscosity does not affect the final configuration reached by the interface. However, it obviously affects the transient phase of the computation before a steady state is reached. If the viscosity of the two fluids is very large, convergence is obtained over long times. On the other hand, in the case of low viscosity, waves may form on the interface that can lead to numeric instabilities. In the course of the simulations, the values of the viscosity of the two fluids were tuned to optimize numeric efficiency and shorten the computational time.

The numeric model described here was previously<sup>12</sup> validated by comparing the numeric solution of the interface between silicone oil and AH in a spherical domain<sup>13</sup> with predictions obtained by a code written ad hoc, with which the shape of the interface was obtained by solving a system of differential equations derived from the Laplace-

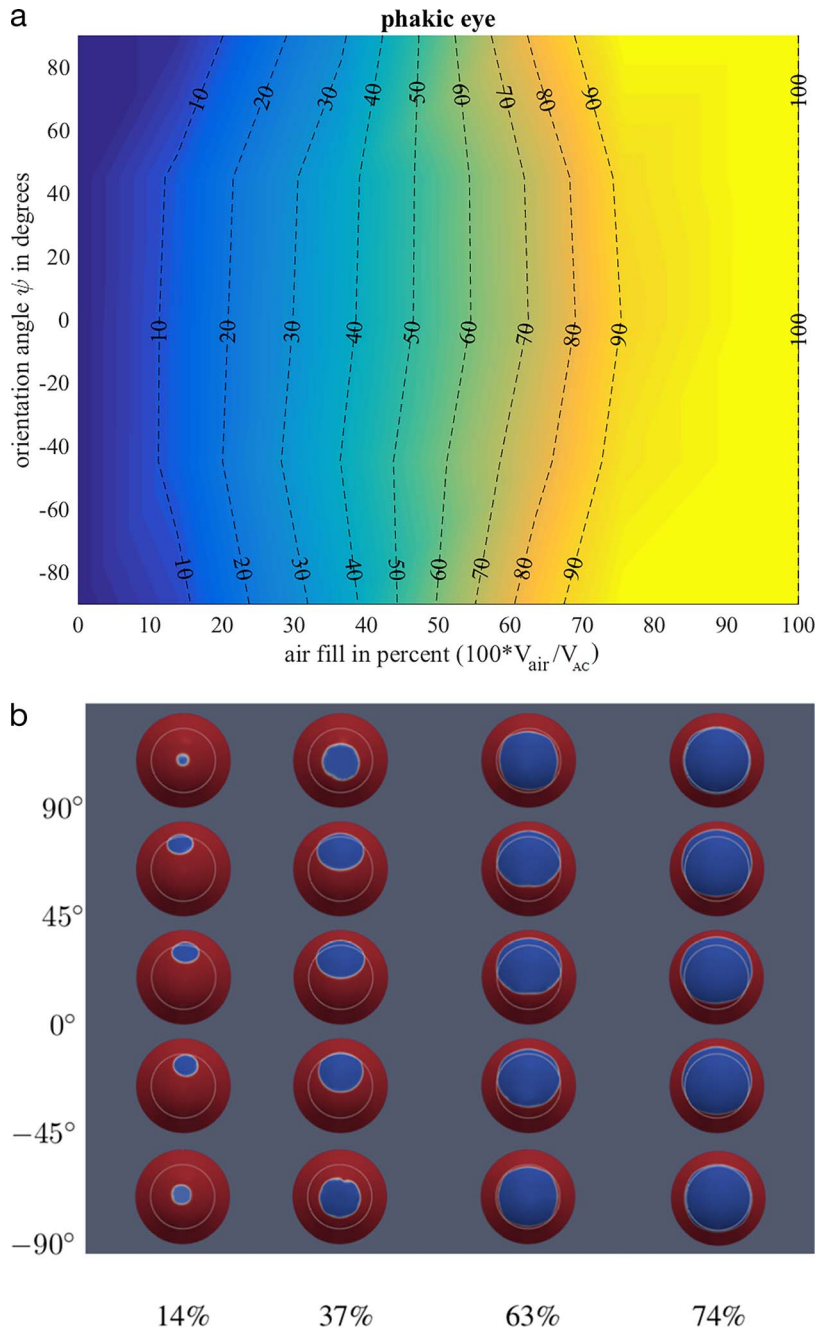


**Figure 6.** (a) Contours of air coverage on the graft  $S_{\text{air}}/S_{\text{graft}}$  (in percent) in the plane  $\varphi - \psi$  (filling ratio – orientation) for the case of a phakic eye with ACD = 2.65 mm. (b) Air coverage on graft of 8.5 mm diameter (gray circle); left to right, gas fill ratio  $\varphi = 14, 37, 63, 74\%$ ; top to bottom, positioning  $\psi = 90^\circ, 45^\circ, 0^\circ, -45^\circ, -90^\circ$ . Air is blue and aqueous humor is colored red.

Young law. There it was shown that the numeric solution perfectly matches the simplified axisymmetric model when the spatial resolution is adequate.

### Parameters and Observables

The effects of different gas filling and patient positioning were analyzed numerically for each AC

using two different gases; air and sulfur hexafluoride (SF6). The properties of aqueous humor, air, and SF6 used here are given in Table 2 including references. The filling ratio was defined as the portion of gas volume with respect to the total AC volume,  $\varphi = V_{\text{gas}}/V_{\text{AC}}$ . The positioning angle  $\psi$  was defined with respect to the direction of gravitational acceler-

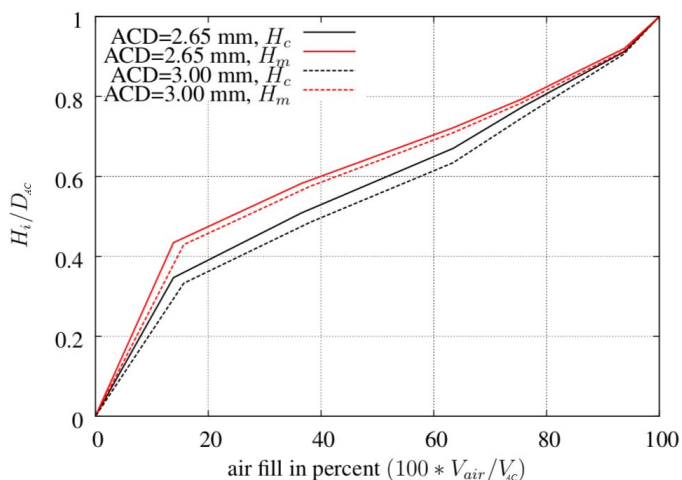


**Figure 7.** Comparison of the vertical gas fill heights  $H_c$  and  $H_m$  normalized with the AC diameter ( $D_{AC}$ ) for phakic ACs with ACDs of 2.65 mm and 3.00 mm (horizontal gaze,  $\psi = 0^\circ$ ). The subscript c refers to the vertical height from inferior gas-cornea contact to superior chamber angle, and subscript m to the vertical height from inferior bubble to superior chamber angle (see Fig. 3). Both heights ( $H_c$  and  $H_m$ ) are calculated relative the AC diameter ( $D_{AC}$ ) and can, therefore, be referred to as height ratios.

ation (Fig. 2). The volume filling ratio  $\phi$  was varied between 0 and 1 and the positioning angle between  $-90^\circ$  and  $90^\circ$  (horizontal gaze,  $\psi = 0$ ). The contact angle  $\alpha_{\text{cornea}}$  for air and SF6 was based on patient measurements with anterior segment optical coherence tomography (AS-OCT, CASIA2) using the angle measure tool in the accompanying viewer software (version 2C). For each patient we used a vertical scan, zoomed in to where the gas bubble departed from the cornea and measured the contact angle at this site. The mean contact angle of the cornea was  $16.6^\circ$  for air (standard deviation [SD] 3.2) and  $16.8^\circ$  for SF6 (SD 3.1) based on measurements from 10 and 14 patients with air and SF6-gas, respectively. From these results it was decided, for simplicity, to fix  $\alpha_{\text{cornea}}$  to  $17^\circ$  for air and SF6 in the numeric analysis. The main interest of the current study was to evaluate the gas-graft coverage, which we defined as the area of gas in contact with the graft divided by the total graft area,  $S_{\text{gas}}/S_{\text{graft}}$ . In our study, we used a graft with 8.5 mm diameter. Since it is not possible to clinically measure the volume of gas used in the AC after endothelial keratoplasty, we evaluated two parameters from the numeric results that can be measured clinically; namely  $H_m$ , which is the vertical height from inferior bubble to superior chamber angle, and  $H_c$ , which is the vertical height from the inferior gas-cornea contact angle to the superior chamber angle (Fig. 3).  $H_c$  and  $H_m$  are height ratios as they are divided by the

height of the AC ( $D_{AC}$ ). The value of  $H_m$  is obtained clinically using a slit-lamp while  $H_c$  is obtained from AS-OCT, and both vertical height ratios are evaluated corresponding to patient looking straight ahead ( $\psi = 0$ ).

## Results

### Validation of the Numeric Model

The numeric model can be validated quantitatively by comparing the values of  $H_c/D_{AC}$  and  $H_m/D_{AC}$  with clinical values obtained for an AC with equal or similar ACD value. Further, a qualitative validation can be made by comparing the intraocular bubble shape. The volume filling ratio  $\phi$  from the clinical case remains unknown and, thus, cannot be used for validation.

As an example, we take a clinically measured gas fill in an AC with  $ACD = 2.75$  mm (Fig. 4c),  $H_c/D_{AC} = 49.4\%$ , and  $H_m/D_{AC} = 58.4\%$ . A numeric solution also was computed on the patient specific AC with  $ACD = 2.75$  mm and the filling ratio matched to  $H_c/D_{AC} = 49.4\%$  (Figs. 4a–b). The resulting filling ratio (i.e., volume fill) was 39.5% and the corresponding  $H_m/D_{AC}$  ratio was 58.4%. Thus, the inferior bubble margin of the clinical case was predicted exactly by the numeric model. This, however, does not imply that the bubble shapes in the two cases are the same. Almost no differences in the bubble curvature are visible in Figure 4c—it is crucial to keep in mind that distortions occur on OCT when imaging through gas, why the images may appear different without being so. Moreover, a front view comparison is shown in Figure 5. Here, the curvature and horizontal extension have a good match with minor differences visible superiorly. Finally, the numeric gas fill in the idealized model (Fig. 1a,  $ACD = 2.65$  mm) also is somewhat comparable: to obtain  $H_c/D_{AC} = 49.4\%$ , a filling ratio of 34.4% is required and the corresponding value of  $H_m/D_{AC}$  is 57.1% (Fig. 7).

### Phakic AC

The contours of gas-graft coverage (in percent) as a function of position angle ( $\psi$ ) and air fill ( $\phi$ ) in the phakic AC ( $ACD = 2.65$  mm) are visualized in Figure 6a.

Figure 6a shows how air fill profoundly affects the gas-graft coverage, while positioning only has a minor role. The strongest variation in gas-graft coverage appears for gas volume fill between 15% and 75%. The small variation of gas-graft coverage with

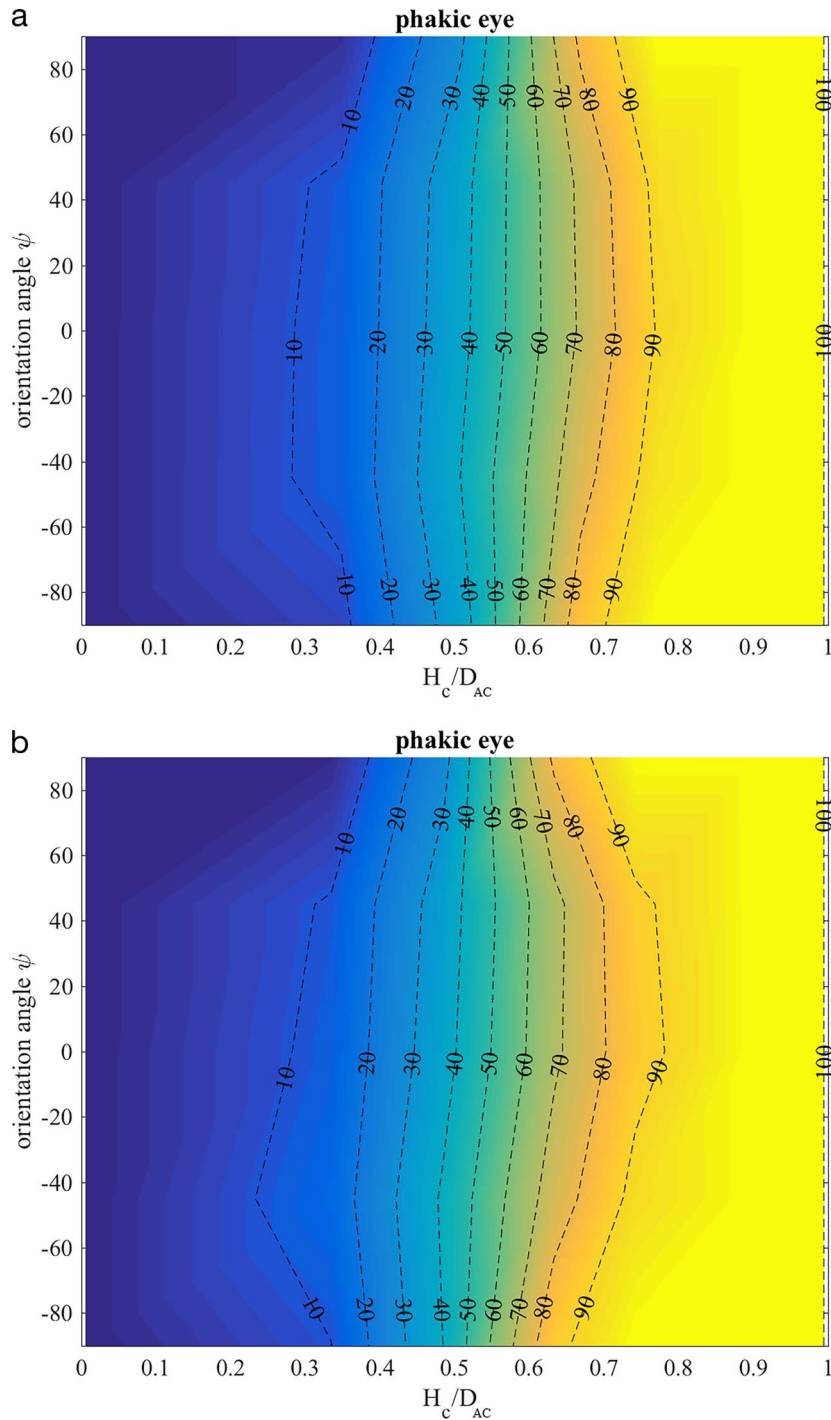


**Figure 8.** Contours of air coverage on the graft  $S_{air}/S_{graft}$  (in percent) in the plane  $H_c/D_{AC} - \psi$  for the case of a phakic eye with ACD = 2.65 mm (a) and ACD = 3 mm (b). Numeric values of the contours in Figure (8a) are found in [Supplementary Table S1](#).

positioning can be explained as follows; when gas fill is  $>50\%$  the slight curving of the contour lines of gas-graft coverage indicates that gas-graft coverage is slightly greater with a patient in the supine position. When gas fill is  $<50\%$  the gas-graft coverage is slightly less in the supine position as opposed to gaze

straight ahead. This is due to gas bubble morphology, as the bubble can be more spherical (smaller surface area) in the voluminous center of the AC while the bubble surface area increases when the bubble distends near the AC angles. [Figure 6b](#) shows the gas-endothelial contact with various gas fills as well as

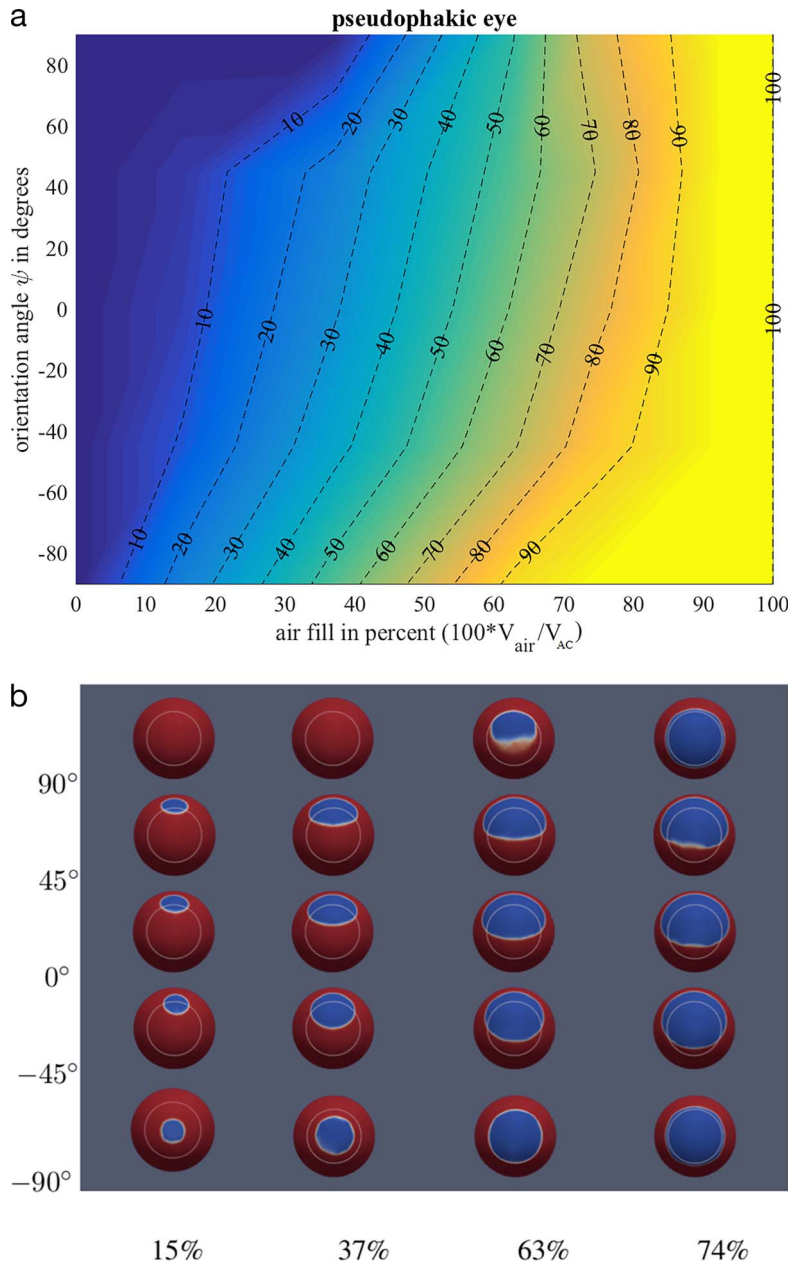


**Figure 9.** (a) contours of air coverage on the graft  $S_{air}/S_{graft}$  (in percent) in the plane  $\varphi - \psi$  (filling ratio - orientation) for the case of a pseudophakic eye with  $ACD = 4.35$  mm. The graph shows how much less air fill is required to achieve a large gas-graft coverage with the face-up position ( $\psi = -90^\circ$ ). (b) Air coverage on graft of 8.5 mm diameter (gray circle); left to right,  $\varphi = 15, 37, 63, 74\%$ ; top to bottom,  $\psi = 90^\circ, 45^\circ, 0^\circ, -45^\circ, -90^\circ$ . Air is blue and aqueous humor is colored red.

with varying directions of gaze. Especially with smaller gas bubbles the location of gas-endothelial coverage is markedly influenced by positioning, whereas larger bubbles vary less in terms of location and amount of endothelium coverage. A gas fill can be expressed in terms of  $H_c$  (measurable with AS-OCT) and  $H_m$  (height seen in slit-lamp). A comparison of the two vertical heights, here normalized with  $D_{AC}$ , is shown in Figure 7.

$H_c$  and  $H_m$  follow an almost linear relation with respect to air fill ( $\varphi$ ) for fills larger than 10%. Moreover, the difference in vertical heights between the two ACs is small. As it is hard to estimate the amount of gas used in the AC volume after endothelial keratoplasty, Figure 8 becomes more practical than Figure 6. Figure 8 confirms the findings of Figure 6, that the dominant parameter affecting graft coverage is the gas fill ( $H_c/D_{AC}$  ratio); especially

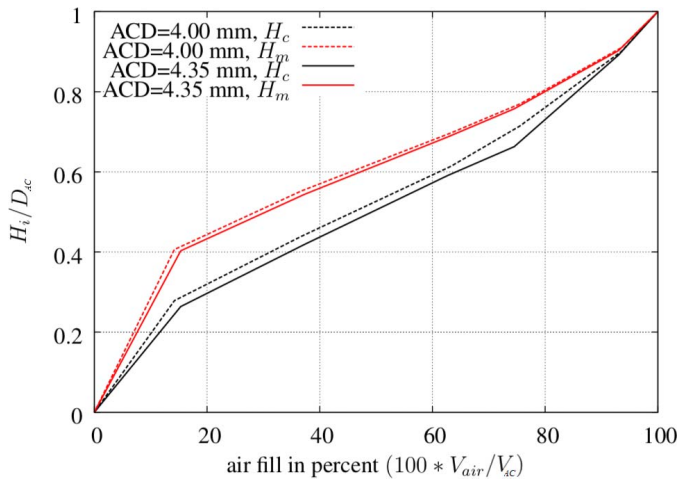


**Figure 10.** Comparison of the vertical heights  $H_c$  and  $H_m$ , normalized with the AC diameter ( $D_{AC}$ ) for pseudophakic ACs with ACDs of 4.00 mm and 4.35 mm, respectively (horizontal gaze,  $\psi = 0^\circ$ ). Again, the subscript c refers to the vertical height from the inferior gas-cornea contact angle to the superior chamber angle and subscript m refers to the vertical height from the inferior bubble margin to the superior chamber angle (see Fig. 3). Both heights ( $H_c$  and  $H_m$ ) are calculated relative the AC diameter ( $D_{AC}$ ) and, therefore, referred to as height ratios.

for  $H_c/D_{AC}$  values between 35% and 75%. Again, only a weak dependency of the surface coverage is found with respect to the orientation angle (i.e., patient positioning; see also Supplementary Table S1).

### Pseudophakic AC

Unlike the phakic cases, in the pseudophakic models with AC depths of 4.00 and 4.35 mm surface coverage have large variations with respect to orientation and air fill (Fig. 9a). In particular, the face-down ( $\psi = 90^\circ$ ) position is much worse concerning the graft coverage compared to the face-up ( $\psi = -90^\circ$ ) position, regardless of air fill. For the case of face-down position ( $\psi = 90^\circ$ ) and air fill below 50%, the bubble is absent. The corresponding corneal endothelium coverage of the air bubble is shown in Figure 9b. Compared to the phakic case, the variation of endothelial gas coverage due to positioning is much more evident in the pseudophakic eye. These large differences are due to larger ACD values (and, thus, a larger AC). When air fill is very high ( $\varphi \approx 90\%$ ), the cornea and iris will be in contact with the bubble and the coverage is similar to the phakic case. As the value of air fill decreases, a large variation of bubble positioning as a function of patient orientation occurs.

Again, we have evaluated the vertical height ratios

$H_c/D_{AC}$  and  $H_m/D_{AC}$  as a function of air fill (Fig. 10). There is a larger discrepancy between  $H_c$  and  $H_m$  in eyes with a deeper AC (compare Figs. 7 and 10). Especially in deep chambers, part of the gas bubble does not contribute to graft contact (e.g., difference between  $H_c$  and  $H_m$  – see Fig. 3) potentially making ideal graft coverage in deep chambers slightly more challenging. When comparing the graft coverage on the two pseudophakic models, especially the case with  $ACD = 4.35$  mm (Fig. 11b) shows clear variations in the gas-graft coverage as a function of the orientation angle. Again, one can contribute this difference to ACD; with increasing value of ACD positioning becomes more crucial (see also Supplementary Table S2).

### Air Versus SF6

The results so far have been shown for the case of air fill. However, several reports have advocated for the use of SF6 due to the suggestion of improved outcomes.<sup>20,21</sup> We compared air and SF6 in a numeric investigation for the case of the phakic model using SF6 ( $ACD = 3$  mm). We parametrically varied the gas fill and orientation angle and measured the surface of gas in contact with the cornea ( $S_{gas}$ ) and normalized the results with the surface of the cornea ( $S_{endothelium}$ ). The results from air and SF6 were almost equivalent (see Fig. 12). The main difference between the properties of air and SF6 is the value of the density,  $1.225$  kg/m<sup>3</sup> for air and  $6.17$  kg/m<sup>3</sup> for SF6. However, from a mechanical point of view, the shape of the AH-gas interface is determined by the density difference,  $\Delta\rho_{gas} = \rho_{AH} - \Delta\rho_{gas}$ . In these cases,  $\Delta\rho_{air} = 998.8$  kg/m<sup>3</sup> and  $\Delta\rho_{SF6} = 993.8$  kg/m<sup>3</sup> and the relative difference is approximately 0.5%. For this reason, surface coverage of gas on the graft after DMEK using air or SF6 can be considered equivalent.

### Central Patch of Aqueous Humor Within the Gas Bubble

During the current numeric study, in some cases a small patch of AH was found centrally between the air bubble and the corneal endothelium, in particular for the cases of the phakic eye model and air filling ranging from 37% to 63%, but also in the pseudophakic model. For air fill increasingly greater than 63%, the patch decreased in size. In Figure 13, the central patch of AH, obtained from a numeric simulation of the patient specific phakic AC, is clearly visualized and found in the proximity of the pupil.

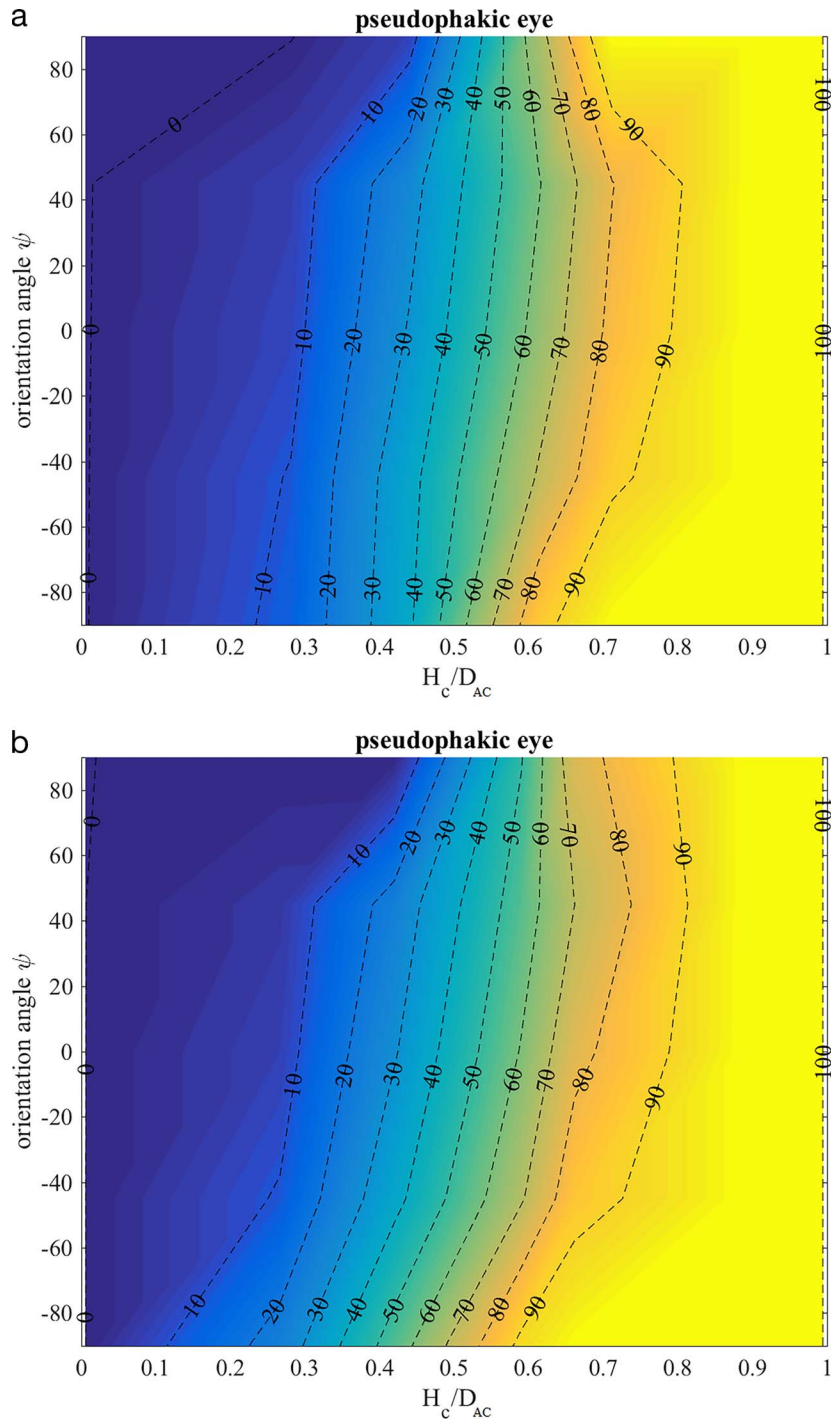


**Figure 11.** Contours of air coverage on the graft  $S_{air}/S_{graft}$  (in percent) in the plane  $H_c/D_{AC} - \psi$  for the case of a pseudophakic eye with  $ACD = 4$  mm (a) and  $ACD = 4.35$  mm (b). Especially (b) shows clear variations in graft coverage as a function of the orientation angle. Numeric values of the contours in (b) are found in [Supplementary Table S2](#).

The patch of AH varied slightly in diameter, but its thickness remained approximately  $30 \mu\text{m}$ . To exclude numeric artefacts, the numeric results were carefully checked by varying the spatial resolution and initial conditions. The patch appears less clearly in the

pseudophakic AC as the radius of curvature of the cornea is smaller compared to the phakic AC. Since the contact angle between AH/air and the cornea is small, approximately 17%, a decrease in the surface curvature will decrease the diameter and thickness of

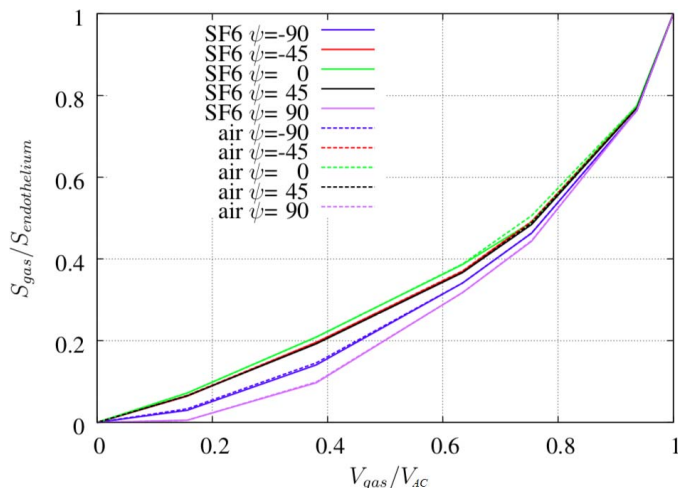


**Figure 12.** Comparison between air and SF6; fraction of gas coverage on the cornea,  $S_{gas}/S_{endothelium}$ , as a function of the volume filling ratio,  $V_{gas}/V_{AC}$ , for different values of the positioning angle  $\psi$ . The values for air and SF6 are nearly identical.

the AH patch. A similar effect is obtained by increasing the AH/air contact angle with the cornea. Results of such analysis are seen in Figure 13, where the value of the contact angle is  $17^\circ$ ,  $25^\circ$ , and  $40^\circ$ , from left to right, respectively. Clearly, as the contact angle is increased the patch becomes smaller. As the main objective of the gas bubble is to apply a support for the graft while healing after DMEK, and the force is proportional to the volume of the inserted gas, it was decided to ignore its effect in this study. Thus, the bubble, when present in the numeric results, was not accounted for when evaluating the graft coverage. Whether it is present clinically or whether there are clinical implications of this fluid patch is uncertain; however, it may aid corneal thinning early in the postoperative period after DMEK.

## Discussion

In the current literature of endothelial keratoplasty, the reported postoperative gas fills have unfortunately been unvalidated and nonstandardized estimations from slit-lamp examination. The difficulty of accounting for the effect of postoperative patient positioning on gas-graft coverage further hinders understanding of gas in the AC. To decipher how gas fill influences DMEK outcome, it is crucial to have standardized and accurate means to measure and understand its morphology in the AC. Untangling the Gordian knot of gas and positioning brings us one step towards a deeper understanding of the

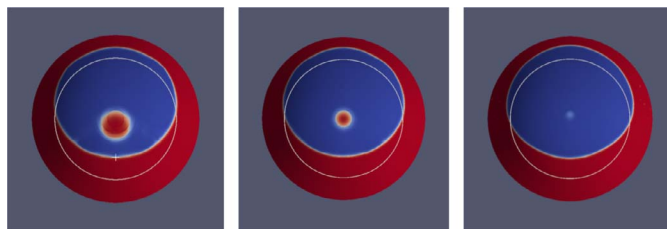


**Figure 13.** Comparison of the central patch of aqueous humor obtained from numeric simulations with 63% air fill and a gaze directed  $45^\circ$  downward ( $\psi = 45^\circ$ ), indicating aqueous humor (red), air (blue) and graft (white). The aqueous humor/air contact angle with the cornea, from left to right, is  $17^\circ$  (nominal),  $25^\circ$ , and  $40^\circ$ , respectively.

DMEK procedure. Gas fill can be measured by: (1) estimation from slit-lamp examination (using  $H_m/D_{AC}$  as  $H_c$  is difficult to visualize in the slit-lamp) and/or (2) by use of AS-OCT (using  $H_c/D_{AC}$  as  $H_m$  is difficult to visualize on AS-OCT). Currently, most evaluations of gas fill are performed clinically in the slit-lamp where reflections from the gas bubble are clearly visible (Fig. 14b), yet this reflection represents neither the section of the bubble in contact with the cornea nor the most inferior margin of the bubble (see also Supplementary Figs. S1a, S1b). We have previously advocated that evaluations of gas fill use anterior segment OCT for objective measures to help surgeons verify gas fill.<sup>22</sup>

With AS-OCT, the inferior gas-cornea contact angle is clearly shown giving a better impression of the gas-graft coverage. Additionally,  $H_c/D_{AC}$  gives a more accurate impression of gas volume; for example, in the pseudophakic eyes a 50%  $H_c/D_{AC}$  fill is approximately a 50% volume fill ( $V_{gas}/V_{AC}$ ), whereas a 50%  $H_m/D_c$  fill is under 30% volume fill. The figures provided in this study (Figs. 7, 10) give clinicians the ability to compare and translate between the two gas fill ratios.

Our results from the numeric model implied that the surgeon can do much more for graft coverage with appropriate gas fill than the patient can with positioning, especially in phakic eyes where the role of positioning has a limited effect on the amount of gas-graft coverage. In eyes with a deep chamber ( $ACD = 4.35$  mm), one can appreciate the benefit of positioning, where a 60% volume fill can either mean 60% (horizontal gaze,  $\psi = 0^\circ$ ) or 90% (face up,  $\psi = -90^\circ$ ) graft coverage. However, the reader must bear in mind that the results presented here are a simple ratio ( $S_{gas}/S_{graft}$ ) and do not fully account for the location of graft coverage (e.g., ensuring coverage of

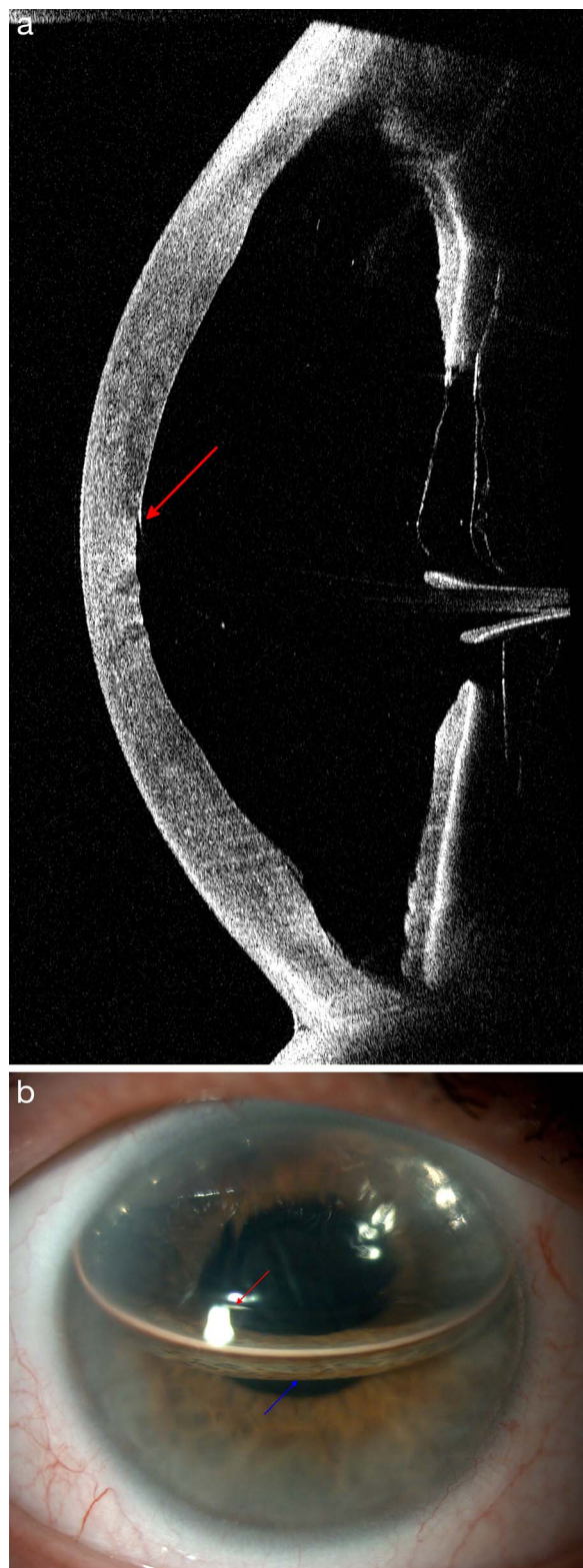


**Figure 14.** (a) OCT image showing inferior gas-cornea contact angle (*red arrow*) used in the height measure  $H_c$ . In this vertical scan the inferior gas-cornea contact angle is midpupillary. (b) In the slit-lamp of the same patient it is difficult to appreciate which

the graft inferiorly) and our theoretical considerations have yet to be validated in a clinical setting.

The main strength of our numeric model is its foundation on physical properties governing gas behavior in the AC, including air and SF<sub>6</sub>s contact angle with the cornea. Furthermore, we compared our numeric model to a patient-specific model for validation. The main limitation of our numeric model is the static and fixed iris. After DMEK, drugs and the gas bubble affect iris shape and, therefore, the shape of the AC. This is especially true in pseudophakic eyes where extraction of the lens leaves ample room for iris mobility. AC depth after DMEK remains rather stable in phakic and pseudophakic eyes – the average maximal range of ACD displacement is 0.29 and 0.40 mm for phakic and pseudophakic eyes, respectively (based on  $n = 5$  patients for both groups). However, for eyes that are made pseudophakic in connection with DMEK (triple surgery), the average maximal range of ACD is 0.77 mm (based on  $n = 5$  patients).<sup>8</sup>

In conclusion, graft coverage in phakic eyes ( $ACD \leq 3$  mm) seems dominated by gas fill and less sensitive to patient positioning. In pseudophakic eyes with larger values of ACD, the graft coverage depends on gas fill and patient positioning, with positioning being even more important as ACD increases. Also, when comparing gas bubbles of equal size, our results demonstrated a negligible difference between the behavior of air and SF<sub>6</sub>. Finally, we advocated the use of AS-OCT for gas fill the as slit-lamp examination can give a misleading impression of gas-graft coverage.

## Acknowledgments

The authors thank Emanuela Mo for preparation of the figures.

Supported in part by CINECA within the ISCRA C project (HP10CHF75B), Rigshospitalets Research Funds, the Synoptik Foundation, and Øjenforeningen, Værn om Synet.

Disclosure: **J.O. Pralits**, None; **M. Alberti**, None; **J. Cabreizo**, None

elements of the gas bubble are in contact with the cornea. The inferior gas-cornea contact angle (*red arrow*) and the inferior bubble margin (*blue arrow*) are highlighted. The space between the *arrows* is without gas-graft contact as the inferior gas-cornea contact angle is midpupillary.

\*JOP and MA contributed equally to this article.

## References

1. Ćirković A, Beck C, Weller JM, Kruse FE, Tourtas T. Anterior chamber air bubble to achieve graft attachment after DMEK: is bigger always better? *Cornea*. 2016;35:482–485.
2. Leon P, Parekh M, Nahum Y, et al. Factors associated with early graft detachment in primary Descemet membrane endothelial keratoplasty. *Am J Ophthalmol*. 2018;187:117–124.
3. Gonzalez A, Price FW Jr, Price MO, Feng MT. Prevention and management of pupil block after Descemet membrane endothelial keratoplasty. *Cornea*. 2016;35:1391–1395.
4. Kopsachilis N, Tsaousis KT, Tsinopoulos IT, Welge-Luessen U. Air toxicity for primary human-cultured corneal endothelial cells: an in vitro model. *Cornea*. 2013;32:e31–35.
5. Landry H, Aminian A, Hoffart L, et al. Corneal endothelial toxicity of air and SF6. *Invest Ophthalmol Vis Sci*. 2011;52:2279–2286.
6. Repetto R, Pralits JO, Siggers JH, Soleri P. Phakic iris-fixated intraocular lens placement in the anterior chamber: effects on aqueous flow. *Invest Ophthalmol Vis Sci*. 2015;56:3061–3068.
7. Kapnisis K, Doormaal MV, Ross Ethier C. Modeling aqueous humor collection from the human eye. *J Biomech*. 2009;42:2454–2457.
8. Alberti M, la Cour M, Cabrerizo J. Air Versus SF6 for Descemet's Membrane Endothelial Keratoplasty (DMEK). <https://clinicaltrials.gov/ct2/show/NCT03407755>; 2016.
9. Helmholtz HV. *Handbuch der Physiologischen Optik*, 3rd ED. Leopold Voss; 1909.
10. Deshpande SS, Anumolu L, Trujillo MF. Evaluating the performance of the two-phase flow solver interFoam. *Comput Sci Discov*. 2012;5:014016.
11. Hirt CW, Nichols BD. Volume of fluid (VOF) method for the dynamics of free boundaries. *J Comp Phys*. 1981;39:201–225.
12. Isakova K, Pralits JO, Romano MR, Beenakker J-WM, Shamonin DP, Repetto R. Equilibrium shape of the aqueous humor-vitreous substitute interface in vitrectomized eyes. *J Model Ophthalmol*. 2017;1:31–46.
13. Eames I, Angunawela RI, Aylward GW, Azarbadegan A. A theoretical model for predicting interfacial relationships of retinal tamponades. *Invest Ophthalmol Vis Sci*. 2010;51:2243–2247.
14. Spandau U, Heimann H. *Practical Handbook for Small-Gauge Vitrectomy*. New York: Springer; 2012.
15. Beswick JA, McCulloch C. Effect of hyaluronidase on the viscosity of the aqueous humour. *Br J Ophthalmol*. 1956;40:545–548.
16. Miyake K, Maekubo K, Miyake S, et al. Measuring contact angles of the lens capsule, collagen type I and collagen type IV. *Eur J Imlant Refract Surg*. 1994;6:132–137.
17. Cunanan CM, Ghazizadeh M, Buchen SY, Knight PM. Contact-angle analysis of intraocular lenses. *J Cataract Refract Surg*. 1998;24:341–351.
18. Wong I, Wong D. Special adjuncts to treatment. In: Ryan S, Wilkinson C, Shachat A, Hinton D, Wiedemann Pain, eds. *Retina*, 5th ed. Philadelphia: W. B. Saunders; 2012:1735–1783.
19. Quiñones-Cisneros SE, Huber ML, Deiters UK. Correlation for the viscosity of sulfur hexafluoride (SF6) from the triple point to 1000 K and pressures to 50 MPa. *J Phys Chem Ref Data*. 2012;41:023102–023102–023111.
20. Güell JL, Morral M, Gris O, Elies D, Manero F. Comparison of sulfur hexafluoride 20% versus air tamponade in Descemet membrane endothelial keratoplasty. *Ophthalmology*. 2015;122:1757–1764.
21. Marques RE, Guerra PS, Sousa DC, et al. Sulfur hexafluoride 20% versus air 100% for anterior chamber tamponade in DMEK: a meta-analysis. *Cornea*. 2018;37:691–697.
22. Cabrerizo J, Alberti M. Anterior chamber gas fill after DMEK. *Cornea*. 2017;36:e23.